Science Advances
AAAS

Supplementary Materials for

Structural basis for sarcolipin's regulation of muscle thermogenesis by the sarcoplasmic reticulum Ca^{2+}-ATPase

Songlin Wang, Tata Gopinath, Erik K. Larsen, Daniel K. Weber, Caitlin Walker, Venkateswara Reddy Uddigiri, Kaustubh R. Mote, Sanjaya K. Sahoo, Muthu Periasamy, Gianluigi Veglia*

*Corresponding author. Email: vegli001@umn.edu

Published 26 November 2021, *Sci. Adv.* **7**, eabi7154 (2021)
DOI: 10.1126/sciadv.abi7154

This PDF file includes:

Figs. S1 to S7
Table S1

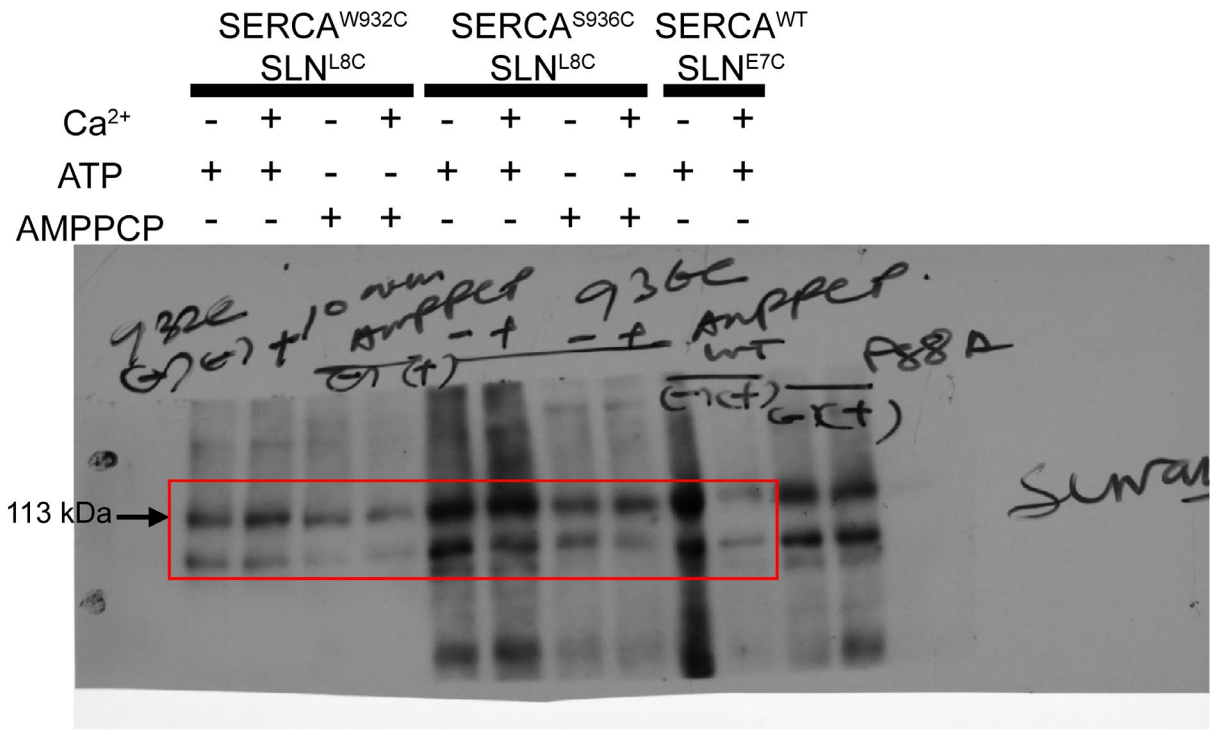

Fig. S1. The full gel image of the cross-linking of SLN^{L8C} with SERCA^{W932C} or SERCA^{S936C}, and SLN^{E7C} with SERCA^{WT} at different conditions. The red square highlights the region we show in Fig. 2G.

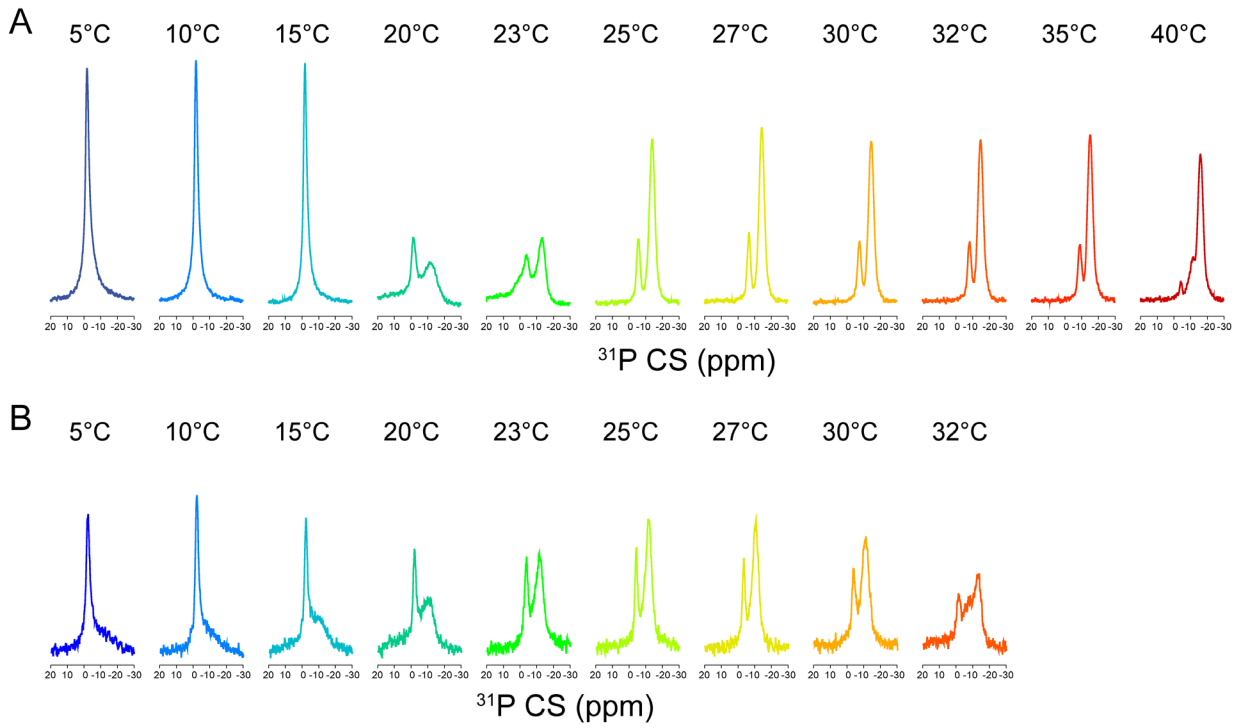

Fig. S2. Monitoring the uniform alignment of the lipid bicelles in magnetic field containing free SLN and the SERCA/SLN complex. One-pulse ^{31}P NMR spectra acquired at different temperatures for bicelles with (A) free SLN, and (B) the SERCA/SLN complex. A 50 kHz SPINAL ^{1}H decoupling was applied during the data acquisition for better resolution. The temperature ranges ideal for the alignment of the lipid bicelles were 24-39°C and 23-31°C for bicelles containing free SLN and the SERCA/SLN complex, respectively. The variable temperature unit was set to 20°C during the execution of the hcSE-SAMPI4 experiments for all SERCA/SLN samples, corresponding to a sample temperature of 26°C as monitored by the ^{1}H chemical shift of the H_2O signal.

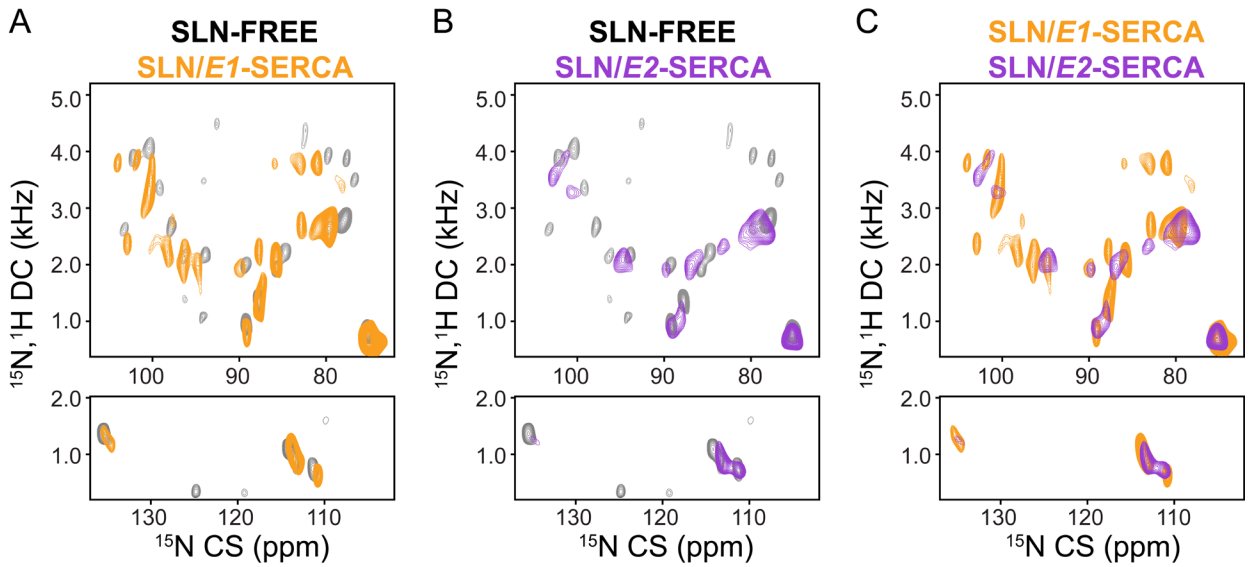

Fig. S3. The comparison of hcSE-SAMPI4 spectra of free SLN, SLN/*E1*-SERCA complex, and SLN/*E2*-SERCA complex. (A) The overlay of hcSE-SAMPI4 spectra of free SLN (grey) and SLN/*E1*-SERCA (orange). (B) The overlay of hcSE-SAMPI4 spectra of free SLN (grey) and SLN/*E2*-SERCA (purple). (C) The overlay of hcSE-SAMPI4 spectra of SLN/*E1*-SERCA (orange) and SLN/*E2*-SERCA (purple).

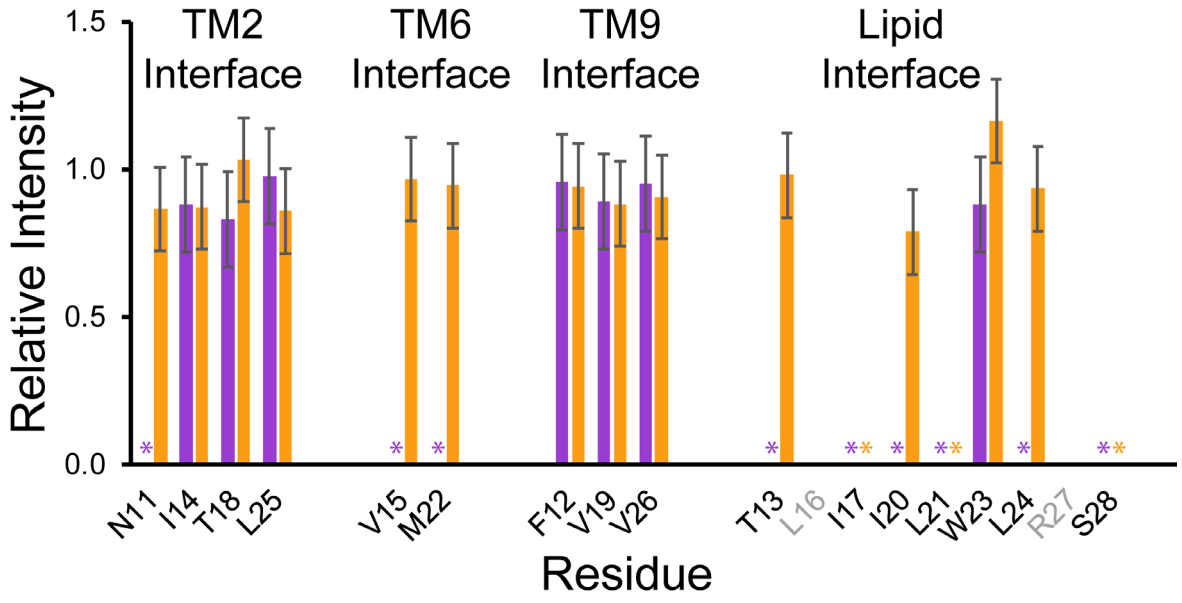

Fig. S4. The analysis of relative peak intensity of SLN upon binding to Ca^{2+} free E2 state (purple) and Ca^{2+} bound E1 state (orange) of SERCA. The peak intensities are normalized by a standard peak to eliminate the uncertainty caused by the variation of the amount of sample. The resonance peak of $R6_{sc1}$ is chosen as the standard peak because it is narrow and intense in both spectra and R6 locates at the SLN/lipid interface thus barely affected by SERCA binding. The residues are organized by the interfaces. The purple or orange asterisks represent the residues which peaks do not appear in the spectrum of *E2*-SERCA or *E1*-SERCA, respectively. The error bars represent the noise level of the spectra. Note that L16 and R27 are excluded due to overlap.

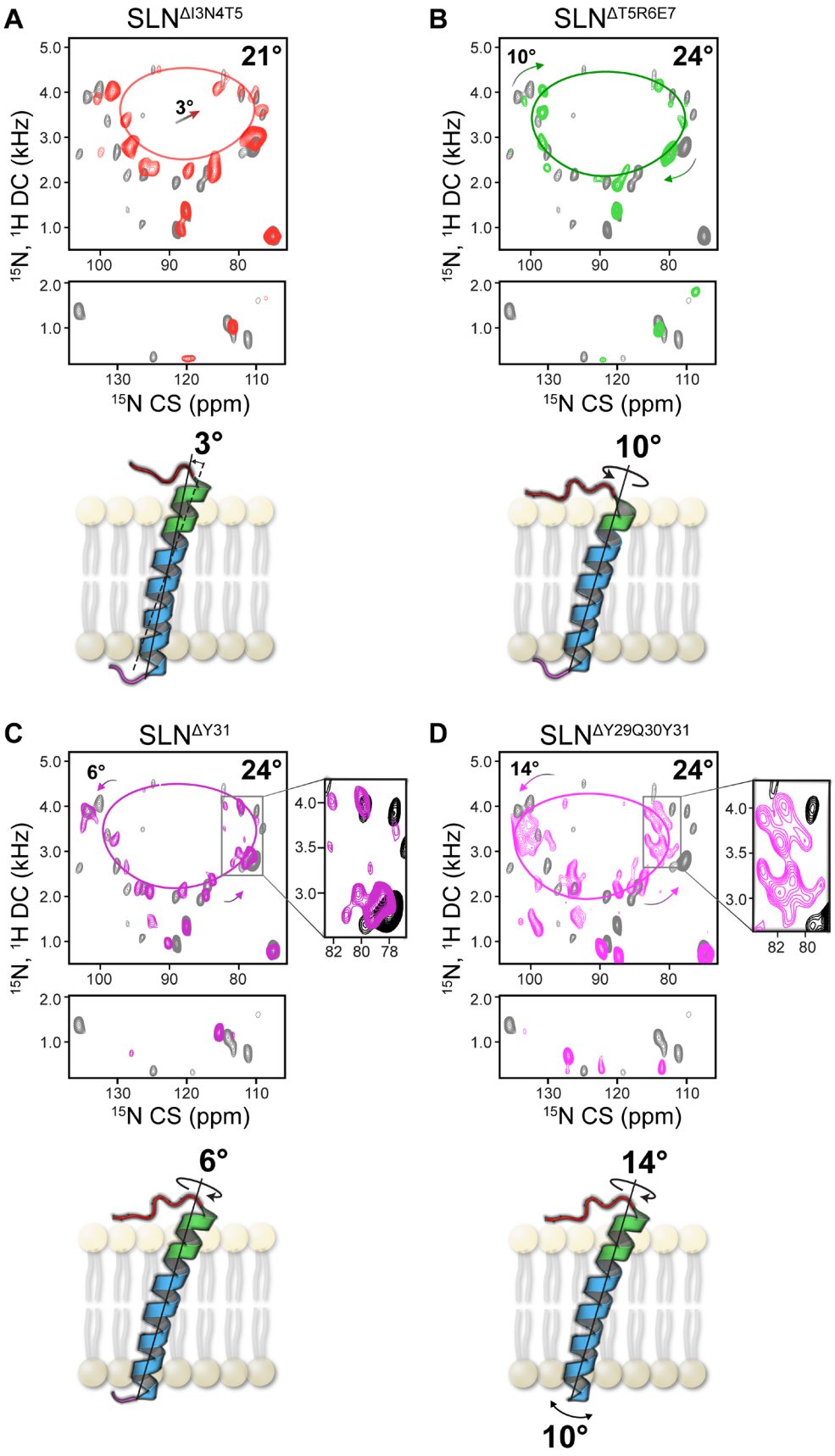
A
SLN^ΔI3N4T5
21°
3°
B
SLN^ΔT5R6E7
10°
24°
^{15}N, ^{1}H DC (kHz)
^{15}N CS (ppm)
3°
10°
C
SLN^ΔY31
6°
24°
D
SLN^ΔY29Q30Y31
14°
24°
6°
14°
10°

Fig. S5. Effects of N-, C-terminal and domain Ib deletions on SLN topology. hcSE-SAMPI4 spectra of $SLN^{\Delta I3N4T5}$ (A), $SLN^{\Delta T5R6E7}$ (B), $SLN^{\Delta Y31}$ (C), and $SLN^{\Delta Y29Q30Y31}$ (D). The hcSE-SAMPI4 spectrum of SLN^{wt} is shown in grey as a reference. The arrows indicate the orientational changes of the SLN topology for the different variants. The spectral insets show multiple populations for selected resonances upon deletion of the C-terminal residues. Cartoon representation of the topological changes of SLN variants is shown below each spectrum.

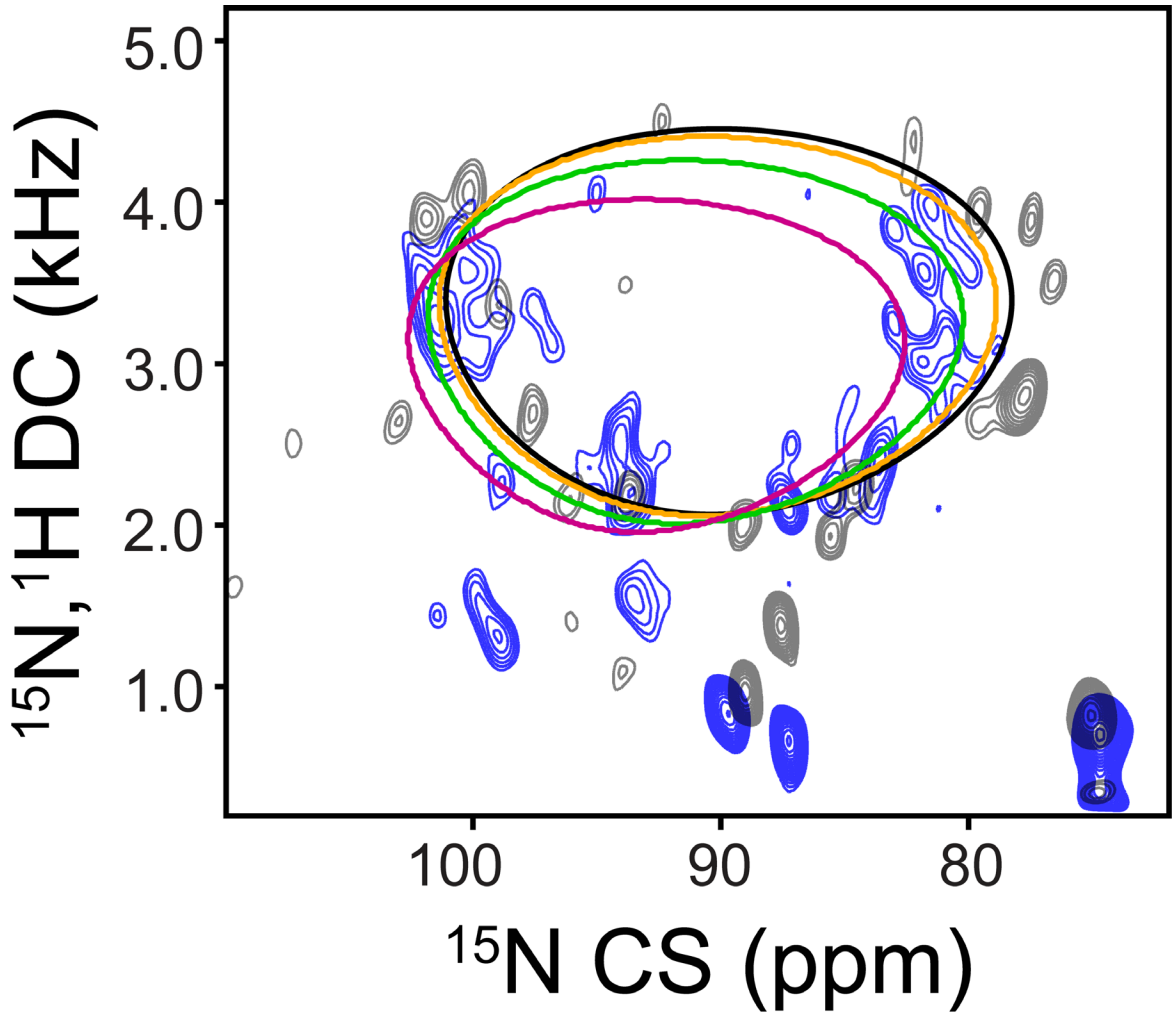

Fig. S6. Simulated PISA wheels for wobbling motion of an ideal helix with tilt axis of ± 0° (black), ± 5° (yellow), ± 10° (green), and ± 15° (magenta) with respect to the bilayer normal. The spectrum of SLN$^{\Delta Y29Q30Y31}$ (blue spectrum) is best fit with a simulated wheel having a wobbling amplitude ± 10°. In contrast, the SLN^{wt} (grey spectrum) is best fit with the simulated wheel without motion.

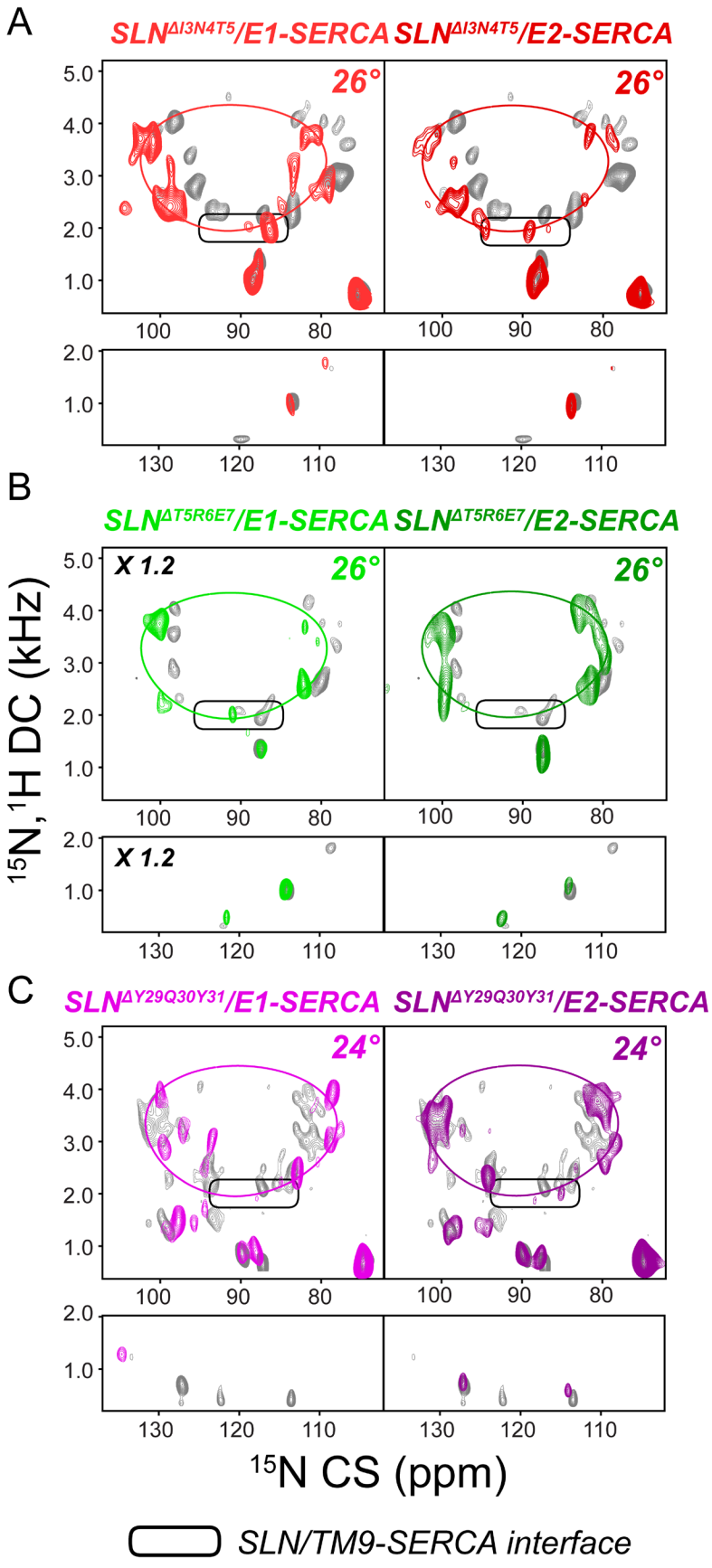
A
SLN^ΔI3N4T5/E1-SERCA
SLN^ΔI3N4T5/E2-SERCA
26°
26°
B
SLN^ΔT5R6E7/E1-SERCA
SLN^ΔT5R6E7/E2-SERCA
X 1.2
26°
26°
X 1.2
C
SLN^ΔY29Q30Y31/E1-SERCA
SLN^ΔY29Q30Y31/E2-SERCA
24°
24°
15N,1H DC (kHz)
15N CS (ppm)
SLN/TM9-SERCA interface

Fig. S7. The hcSE-SAMPI4 spectra of A. SLN$^{\Delta I3N4T5}$, B. SLN$^{\Delta T5R6E7}$, and C. SLN$^{\Delta Y29Q30Y31}$ upon binding to the *E1*-SERCA (left) or the *E2*-SERCA (right). The hcSE-SAMPI4 spectra of free SLN$^{\Delta I3N4T5}$, SLN$^{\Delta T5R6E7}$, and SLN$^{\Delta Y29Q30Y31}$ are shown in gray for comparison. The lowest contour level is set as 5 times of the noise level for all spectra except the SLN$^{\Delta T5R6E7}$/*E1*-SERCA. In this case, the lowest contour level is set as 4.16 times of the noise level due to relatively low sensitivity. The black squares highlight the SLN/TM9-SERCA interface.

Table S1. The effect of truncations on SLN inhibitory function of SERCA. Values for pK_{Ca} were obtained from a fitting of Hill equation using standard coupled enzymatic assays. Error was extracted from fitting. Values of HRR were obtained from four independent ITC titrations for each condition. Error was the standard deviation of the four measurements. The curves of coupled enzymatic assays and ITC titrations are shown in Fig. 2

	pK_{Ca} (I.U.)	HRR (μJ/s)
SERCA	6.76 ± 0.03	3.91 ± 0.12
SERCA/SLN^{wt}	6.58 ± 0.02	5.17 ± 0.06
SERCA/$SLN^{\Delta I3N4T5}$	6.62 ± 0.02	5.19 ± 0.07
SERCA/$SLN^{\Delta T5R6E7}$	6.73 ± 0.03	3.88 ± 0.08
SERCA/$SLN^{\Delta Y29Q30Y31}$	6.72 ± 0.03	4.54 ± 0.26
SERCA/$SLN^{\Delta Y31}$	6.62 ± 0.03	4.97 ± 0.05